ANALYSIS OF STRUCTURAL PARAMETERS OF FOREST TYPOLOGIES USING L-BAND SAR DATA

Análise dos parâmetros estruturais de tipologias florestais utilizando dados SAR em banda L

IGOR DA SILVA NARVAES[1]
JOÃO ROBERTO DOS SANTOS[1]
ARNALDO DE QUEIROZ DA SILVA[1]

National Institute for Space Research – INPE/MCT
Av. dos Astronautas, 1758.
CEP: 12.227-010 - São José dos Campos, SP – Brasil
email: {igor, jroberto, arnaldo}@dsr.inpe.br

ABSTRACT

The main objective of this work is the investigation of the relationship between the polarimetric L-band backscatter (σ^o) from different incidence angles (collected by the airborne sensor R99-B/SIPAM) and the structural parameters of the primary and secondary forest typologies. The area under study is located at the Tapajós National Forest and surroundings (Pará State, Brazil). Using the Freeman-Durden target decomposition technique, the basic backscatter mechanisms are presented to verify the contributions of the physiognomic-structural components of these forest stands in the L-band signal responses. As a conclusion, it is possible to verify that the variable "tree height" has better relations with the backscatter values, when compared to other structural variables, especially when the model also includes variations of the incidence angle of the stripes imaged. The Freeman-Durden decomposition technique indicates that the volumetric scattering component has the strongest influence on the L-band at primary and secondary tropical forests at incidence angles between 52 and 70 degrees, mainly due to the high incidence angle and, consequently the low depth vertical penetration.

Keywords: Forest Inventory; L-Band; SAR Data; Mapping; Tropical Forest; Amazon.

RESUMO

O objetivo principal desse trabalho é investigar a relação entre o retroespalhamento (σ°) de dados SAR polarimétricos de banda L, em diferentes ângulos de incidência (coletado pelo sensor aerotransportado R99-B/SIPAM) e os parâmetros estruturais de sítios de floresta primária e sucessão secundária. A área selecionada para esse estudo está localizada na região da Floresta Nacional do Tapajós (Estado do Pará, Brasil) e áreas circunvizinhas. É utilizada a técnica de decomposição de alvos de Freeman-Durden na avaliação dos mecanismos básicos de espalhamento, para verificar a contribuições das componentes fisionômico-estruturais dos alvos florestais na resposta-radar de banda L. Como conclusão, é possível verificar que a variável "altura das árvores" teve melhor relação com os valores de retroespalhamento, quando comparado com outras variáveis biofísicas, especialmente quando o modelo também incluiu variações do ângulo de incidência na direção em *range*. A técnica de decomposição de Freeman-Durden indicou que a componente volumétrica de espalhamento tem uma forte influência na resposta em banda L para florestas tropicais primárias e secundárias,em ângulos de incidência entre 52 e 70 graus, devido principalmente ao elevado ângulo de incidência e, consequentemente a baixa profundidade de penetração vertical da onda incidente.

Palavras-chave: Inventário Florestal; SAR; Banda L; Mapeamento; Floresta Tropical; Amazônia.

1. INTRODUCTION

The knowledge of the interaction mechanisms between SAR (Synthetic Aperture Radar) signals and the structural properties of forests was investigated in the several studies (VAN ZYL *et al.*, 1987; KASISCHKE *et al.*, 1997; CHAMPION *et al.*, 1998; COOPS, 2002; NEEFF *et al.*, 2005). Characteristics of forest coverage (e.g. density, orientation, shape, dielectric constant, height), terrain aspects (roughness), soil conditions (moisture content, grain size) and also, the aspects of SAR imaging (polarization, incidence angle and wavelength) are important to determine the backscattered signal to the SAR antenna. There are several interaction mechanisms of the radar signal with forest targets, such as: multiple backscatter within the canopy (volumetric scattering), direct scattering from the tree trunks, scattering from the interaction canopy-soil, scattering from the interaction trunk-soil (double bounce), whose intensities depend on the SAR wavelengths, on the polarization, on the angle of incidence and on the terrain parameters. (CLOUDE and POTTIER, 1997; FREEMAN and DURDEN, 1998) According several studies (SAATCHI *et al.*, 1997; HOEKMAN and QUIÑONES, 2000; SANTOS *et al.*, 2002), SAR data are also used to model forest volume and biomass estimation, using the polarimetric backscatter attributes. Depending on the frequency of the sensor, there is a saturation of radar signal for those areas with high biomass concentration. Due to that, estimation models are being improved with SAR interferometric variables (BALTZER, 2001; TREUHAFT *et al.*, 2006;

HAJNSEK *et al.*, 2009). Studying the values of backscatter features (σ^0), the penetration capacity and the predominant scattering mechanisms on vegetation as well as biomass evaluation from multi-frequency and multi-polarized AIRSAR data, it was verified that bands P_{HV} and L_{HV} are more sensitive to the total biomass, presenting furthermore a strong relation with some structural forest parameters such as height (H), basal area (G), and diameter (DBH) (MOUGIN *et al.*, 1999). Nevertheless variations in the floristic composition, forest structure and management practices can have an important effect on the results (HOEKMAN and QUINÕNES, 2000). The high correlation among biomass and L- σ^0_{hh} and σ^0_{hv}, saturated at 100ton/ha for both polarizations was found by WATANABE *et al.* (2006) at a temperate coniferous forest. The same authors, using the target decomposition of Freeman and Durden (FREEMAN and DURDEN, 1998) to generate a scattering model of each tree component, where volume scattering is around 80-90%, when the biomass exceeds 50 ton/ha. For younger stands the component of surface scattering is of around 20%, and the volumetric scattering components are below 70%. Yet, in according to WATANABE *et al.* (2006), the origin of the dependency among the forest species was examined for the σ^0_{HH}– above-ground biomass. It is concluded that a possible cause of the dependency is the different characteristics of the stands rather than forest species.

The objective of this research is to analyze the relation of the L-band scattering with structural aspects from primary forest and secondary succession stages, including the effect of the variations of the incidence angle on the response of the investigated forest targets. Additionally an analysis is made on the contribution of the scattering mechanisms on the forest targets using the Freeman-Durden decomposition technique. The selected area under study is located in the region of Tapajós (Brazil), with the geographical coordinates S 3º 01' 59.85" to S 3º 10' 39.33" and WGr 54º 59' 53.08" to WGr 54º 52' 44.96".

2. MATERIAL AND METHODS

In this study we used polarimetric L-band SAR images, obtained during an airborne campaign with the radar sensor R99-B/SIPAM at HH, VV and HV polarizations and spatial resolution of 5 m. The SAR-R99 data were initially radiometrically calibrated: 1st antenna pattern correction to remove gain variations in the range direction using a polynomial function to fit the sum of the amplitude values; and 2nd absolute calibration, based on the 12 corner reflectors placed in the area under study during the imaging campaign, to allow the transformation of amplitude data in backscatter values of targets, using the method of peak power (GRAY et al., 1990). For the absolute SAR calibration, the average error was -0.8443 dB and the standard deviation 0.18 dB. The σ^0 values at different polarizations were obtained taking into account the average of pixels available at each ROI (sample area), which correspond to the same plots inventoried during the field survey. In the SAR image, the ROI area includes the sample dimension with a

sufficient amount of pixels representative for the theme, reducing so the statistical uncertainties and the influence of speckle noise (WATANABE et al., 2006).

The evaluation of the basic scattering mechanisms was done using the polarimetric decomposition technique of Freeman-Durden, for the incoherent targets, applied to the complex images, which allows estimating the absolute contribution from each one of three physical mechanisms (double-bounce, surface and volumetric scattering). For volume scattering, it is assumed that the radar return is from a cloud of randomly oriented, very thin, and cylinder-like scatters (Li-wen et al., 2007); double-bounce conditions is modeled by scattering from a dihedral corner reflector, where the reflector surface can be made of different dielectric materials; surface scattering is derived by a first-order Bragg modeling. According to FREEMAN and DURDEN (1998), the scattering contribution is obtained by the following expressions:

$$\left\langle |Shh|^2 \right\rangle = fs|\beta|^2 + fd|\alpha|^2 + fv \tag{1}$$

$$\left\langle |Svv|^2 \right\rangle = fs + fd + fv \tag{2}$$

$$\langle ShhSvv* \rangle = fs\beta + fd\alpha + fv/3 \tag{3}$$

$$\left\langle |Shv|^2 \right\rangle = fv/3 \tag{4}$$

The three-component scattering model based on covariance matrix has been successfully applied to decompose polarimetric SAR image (Zhang et al., 2008), under the reflection symmetry condition:

$$\langle ShhShv* \rangle = \langle ShvSvv* \rangle = 0. \tag{5}$$

The final scattering contribution is obtained whether double-bounce or surface scatter is the dominant contribution in the residual, based on the sign of the real part of (Shh S*vv). If Re (Shh S*vv) is positive, the surface scatter is dominant and fix α = -1 .If Re (Shh S*vv) is negative the double- bounce scatter is dominant in the remainder and fix β =1.Then fs, fd and β or α can be estimated from the residual radar measurements. This approach will obviously work best when either *fs* or *fd* are close to zero, or when α or β are close to -1or +1.

Finally, the authors estimate the contribution of each scattering mechanism to the span P, as following:

$$P = P_S + P_d + P_v \equiv (|S_{hh}|^2 + 2|S_{hv}|^2 + |S_{vv}|^2) \quad (6)$$

with

$$P_S = f_S (1 + |\beta|^2) \quad (7)$$

$$P_d = f_S (1 + |\alpha|^2) \quad (8)$$

And

$$P_v = 8^{f_v} / 3 \quad (9)$$

where *fv*, *fd* and *fs* are the contributions to the power from volume, dihedral, and surface scattering, respectively. Additionally, the coefficient α and β are the parameters that can be estimated from some forest variables, such as trunk radius and tree number density. According VAN ZYL (1989), it enables us to identify the contribution of each scattering mechanism only from SAR polarization data, without any field data. Applying this technique we obtained the percent values of the scattering mechanisms over each of the sampled areas (ROI).

The biophysical parameters were collected in 5 areas of primary forest (each plot = 2,500 m2) and 8 areas of secondary succession (each plot = 1,000 m2), positioned geographically with a GPS. It is import to inform that height (H) and diameter at breast height (DBH) measure, which allowed generating the basal area and biomass values of the secondary succession, were collected during 2002. At this specific case of regrowth, in order to reduce the effect of the time imbalance between the field survey (2002) and the SAR imaging (2005), a correction factor was applied to the field inventory data, calculated on the average intervals of tree height and diameter. Such stratification was defined considering the height and DBH intervals from 3 m and 3 cm for the secondary succession respectively. This allowed establishing the average yearly increment by class of interval, considering the recovery age of each plot of secondary succession. The specific allometric equations for biomass estimation for the primary forest (BROWN et al., 1989) and secondary successions (UHL et al., 1998) were used.

3. RESULTS AND DICUSSIONS

3.1. Backscatter versus biophysical parameters

Table 1 presents the radar polarimetric responses, and also the potential scattering mechanisms presented by primary forest (PF) and secondary succession (SS) samples, including its biophysical parameters. Those areas of primary forest present σ^0hh = -7.51 dB± 3.34, σ^0hv = -12.25dB ±3.15 and σ^0vv = -7.53dB ± 3.24;

secondary succession areas, which represent intermediate and advanced phases (characterized by the old regeneration age and also by the vertical structure) present σ^0hh = -7.38 dB± 2.34, σ^0hv = -11.95dB ± 2.27 and σ^0vv = -7.06dB ± 2.29. The values found in this study are coherent with those obtained by Hoekman and Quiñones (2000), SAATCHI et al. (1997), SANTOS et al. (2002), whose variability can be attributed to general differences in the horizontal and vertical structure of the strata from the forest typologies. This also shows that the sensor SAR-R99B presents an adequate radiometric response.

The analysis of the backscattering, for both primary forest and secondary succession samples, shows that there are, in most of the cases different values for the co-polarizations and a stronger backscatter at VV and HH than HV. The return signal is more reduced at the cross-polarization, which is more sensitive to volumetric scattering (random distribution of branches, twigs and leaves. The relation between polarizations and biophysical parameters was evaluated by simple linear regressions.

The analysis of the backscatter of the 13 ROI_S considers not only the physiognomic-structural characteristics of the forest types, but also the incidence angle (Θ) of the imaging. Since the imaging swath of the SAR R99-B was of 30 Km, and the incidence angle varies between 52. and 70.1°, the sampled plots are located, from near to far range between 57° and 65° (Table 1). There is a little increase tendency of $\sigma°_{HH}$ and $\sigma°_{VV}$ with the increment of the Θ value. A possible explanation for this phenomenon is related with the combination to the radar wavelength, polarization and incidence angle. According to VAN DER SANDEN (1997) the L-band interact more with the primary branches and secondary branches and tree trunks – wavelength effect – for the polarization state the $\sigma°_{HH}$ and $\sigma°_{VV}$ have high interaction with the horizontal components in the crown to the secondary forests which are in more dense in general and vertical components (mainly trunks) at the primary forests. However, it interactions is controlled mainly by the low incidence angles which maintain the waves (L-band) interaction on the random scattered elements (branches) in the different crown strata of primary and secondary forest, as proved to the same authors which say "the depth of vertical penetration (δ_p) will decrease with an increase in incidence angle (θ_{inc})". The most relevant volumetric scattering (primary and secondary forests) and double-bounce mechanisms (mainly in primary forests) are due to the combination of those effects cited in this paragraph.

Table 1 - Coherent and incoherent attributes SAR L-band data for sites and respective biophysical parameters of forest typologies.

	Plots	Basal Area (m^2/ha)	Height (m)	Density (ind./ha)	Biomass (ton/ha)	N° pixels	θ	σ°_{vv}*	Stdev	σ°_{hv}*	Stdev	σ°_{hh}*	Stdev	Scattering components Pd** (%)	Pv** (%)	Ps** (%)
SS	1	14.11	10.14	920	60.21	3276	57.38	-9.698	2.640	-14.423	2.603	-9.395	2.665	1.59	95.04	3.38
	2	15.54	11.10	1510	66.17	3710	58.17	-6.622	2.161	-11.462	2.114	-6.968	2.196	1.55	95.53	2.93
	3	11.87	11.81	1040	51.32	3078	63.64	-6.948	2.437	-12.714	2.277	-8.319	2.439	2.19	93.71	4.11
	4	11.07	11.66	1160	47.53	3021	63.48	-6.835	2.103	-11.633	2.269	-6.916	2.264	1.30	95.47	3.23
	5	10.34	12.75	980	46.23	3325	65.54	-6.295	2.204	-10.903	2.128	-6.268	2.305	1.51	95.14	3.35
	6	6.61	12.52	630	30.96	6902	60.41	-6.786	2.114	-11.532	2.063	-7.217	2.112	1.39	95.75	2.86
	7	21.08	15.38	1228	111.00	6811	60.25	-6.504	2.344	-11.407	2.345	-6.973	2.359	1.55	95.12	3.33
	8	27.00	13.85	452	131.99	3923	60.29	-6.779	2.357	-11.490	2.377	-6.983	2.380	1.28	95.58	3.14
PF	9	32.38	12.01	1176	269.37	6883	59.52	-7.512	3.095	-12.172	3.036	-7.707	3.192	1.38	95.67	2.95
	10	29.44	11.29	1220	248.16	3129	57.7	-8.743	3.279	-13.211	3.153	-8.703	3.418	1.49	95.20	3.32
	11	29.88	12.72	420	263.32	2131	57.12	-8.263	3.244	-13.106	3.124	-8.100	3.249	1.57	94.67	3.76
	12	18.74	17.81	432	194.33	3603	65.72	-6.301	3.162	-11.122	3.079	-6.161	3.314	1.14	95.36	3.50
	13	14.53	15.79	460	122.60	5441	62.91	-6.812	3.412	-11.633	3.362	-6.868	3.534	1.39	95.74	2.87

PS: The incoherent attributes* is based only in the measures of radar power, while the coherent attributes** aggregate the beyond it the phase (HENDERSON and LEWIS, 1998).

Table 2 shows the R^2 values and one verifies that the variable "tree height" (average height values of trees within the stand of each plot) presented solely the best relation with the σ^0_{hh} when compared with the other biophysical variables. Generally the tree height is correlated positively with the forest biomass and volume till the saturation point. This indicates that the higher the trees and the larger the canopies, the stronger is the amount of scattering elements in the resolution cell (ROI) and consequently there is a higher backscatter, at a positive correlation. However, this variable must be evaluated jointly with incidence angle. The relation between σ^0_{hh} and tree height tends to be high due mainly to the low capacity the wave penetration because of the high incidence angle, thus the interaction tends to happen in the canopy. According to VAN ZYL *et* al. (1987) in this situation, the attenuation by the canopy is stronger and thus single and double scattering is reduced and volume scattering dominates.

Table 2 - Coefficient of determination (R^2) among structural aspects and backscatter coefficients.

Variables	L_{hh}	L_{hv}	L_{vv}
Density (N ha^{-1})	0.0320	0.0037	0.0025
Basal area (m^2 ha^{-1})	0.0654	0.0672	0.1186
Tree height (m)	**0.4380**	**0.3384**	**0.3276**
Diameter (cm)	0.1106	0.0631	0.0500
Biomass (ton ha^{-1})	0.0355	0.0541	0.1036

Due to the importance of the incidence angle (Θ) the evaluation of backscatter was also done together with the biophysical parameters (Table 3) by multiple regression. The choice of the parameters was made considering the correlation matrix of the total from independent variables, jointly with the construction model for the multiple regression of best subsets, based on choice criteria R^2, R^2 adjusted and Mallows' Cp. Based on the mentioned statistical test, the backscatter are best explained by the vertical structure (log H) of the forest type and by the incidence angle. For a 90% level of trust, the best fit was obtained for polarization HH (R^2 = 0.59).

Table 3 - Relation model between backscatter and tree height variables, including the sar incidence angle. The values in bold are significant due to the p-value, at a 90% level of trust.

		y =a + b log (H) + c (Θ)			
α = 0.10		a	b	C	R^2
σ°	HH	-22.4537	2.7171	0.1330	0.59
	p-value		**0.0882**	0.1035	
	HV	-26.7827	2.4601	0.1387	0.50
	p-value		0.1782	0.1446	
	VV	-23.3894	2.0736	0.1784	0.56
	p-value		0.2307	**0.0592**	

IMHOFF *et al.* (1986) and AIBA *et al.* (1988) demonstrated the importance of the incidence angle for the penetration of microwaves in tropical forests at L-band. Both studies analyze the penetration with incidence angles ranging from 35° to 55° in forest typology. The results found however differ among each one: while IMHOFF *et al.* (1986) report that the δ_p may be as much 12.5 m at much lower incidence angle, AIBA *et al.* (1988) report a δ_p approximately 6 m to the same incidence angle. According to VAN DER SANDEN (1997), differences in depth of

vertical penetration – in this case, related to the tree height – affect the interaction of the microwaves with the forest because the processes of transmission, scattering and absorption that occur in different parts of the volume and/or different surfaces.

An additional analysis on the influence of the vertical structure (height class intervals) from the forest cover and of the similar incidence angle (Θ) on the Sigma Nough (σ^0) values is done in this study. At Figure 1, one observes an example of tree stratification by height intervals for three samples of primary forest and secondary succession. Considering the configuration of these samples, they present all a similarity between plots 10 and 11 (primary forest), although the plot 1 (secondary succession) has on the distribution of trees by strata substantially different. For those cases of very high incidence angles, the backscatter values in different polarizations are quite similar related to the same structural characteristics. However, when we have difference in the forest succession, in other words, on the vertical structure distribution, the backscatter values are superior to the primary forests due mainly to the close forest crown. This fact does not occur when there are differences at the incidence angle, with a quite increase on the σ^0 values at higher incidence angles, as mentioned previously.

Figure 1 - Diagram of DBH variable of primary forest samples and respective backscatter values associated to the SAR incidence angles.

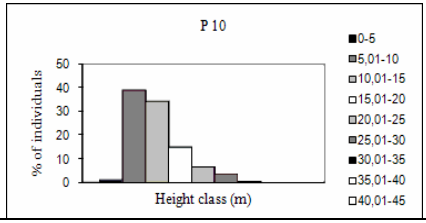

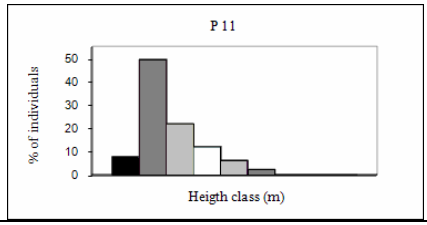

θ = 57°.7; L_{VV}= -8.743; L_{HV} = -13.211; L_{HH} = -8.703

θ = 57°.12 L_{VV} = -8.263 L_{HV} = -13.106 L_{HH} = -8.100

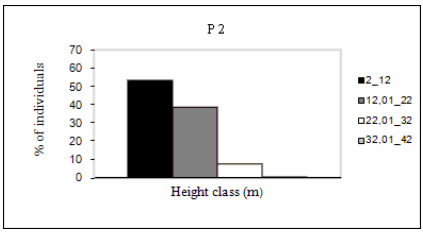

θ = 58°.17 L_{VV} = -6.622 L_{HV} = -11.462 L_{HH} = -6.968

3.2. Contribution of the scattering mechanisms

Using the Freeman-Durden decomposition, it was possible to verify the contribution of the three components of the scattering mechanism (surface, double-bounce and volumetric) for each one of the ROIs, representing primary forest and the secondary succession stages (Figure 2). The model indicated (Table 1) that volume scattering is a dominant component and accounts for 93.71 - 95.75% of the total scattering, on both primary forest types and intermediate/advanced recovery stages. Double-bounce scattering components present values between 1.14 - 2.19% of the total scattering and the surface scattering corresponds to 2.86 - 4.11% of the total. It is important to mention that the surface scattering fraction presents values slightly above those of the double-bounce component. The inversion of the performance from these two last scattering mechanisms, specifically in tropical forests, can be due to high incidence angles (Θ) and consequently low depth vertical penetration (VAN DER SANDEN, 1997), because higher incidence angles favor the specular reflection.

Figure 2 - Freeman-Durden decomposition showing the color image derived from P_d (red), P_v (green), and P_s (blue), where P is a measured power decomposed into three quantities: *d* = double-bounce, *v* = volumetric; and *s* = surface scatters.

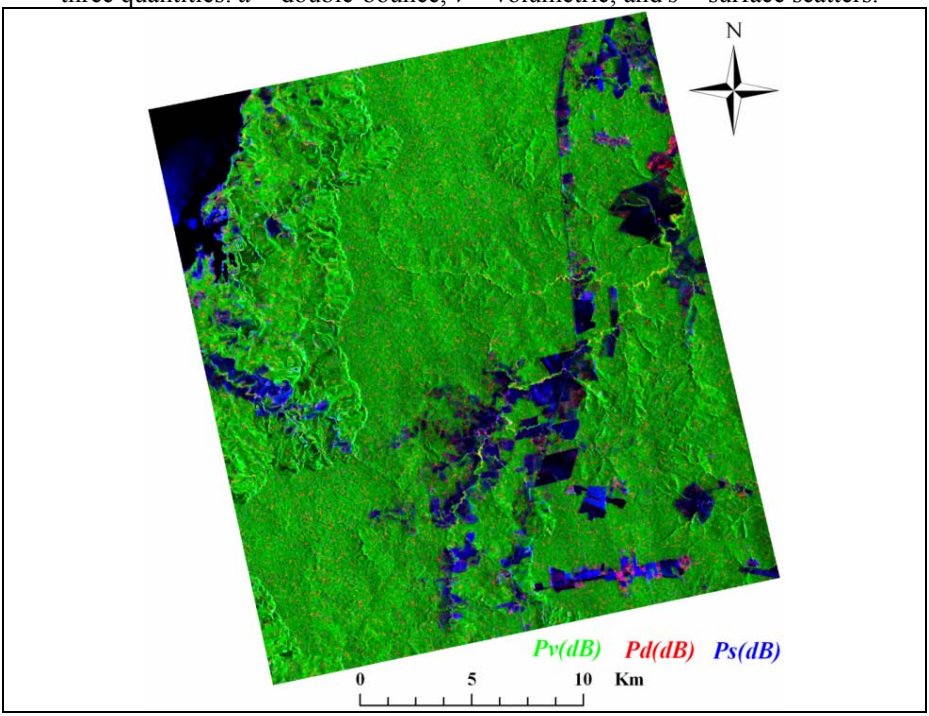

Analyzing the forest structure dependency of the relation between L-band (ALOS/PALSAR) σ° and biophysical parameters of four types of coniferous and some broadleaf stands, WATANABE *et al.* (2006) applied the Freeman-Durden technique and found the same relation as we did in this work. In other words, the surface scattering are superior to double-bounce scattering, with incidence angle more grazing than in this work. The same authors concluded that this characteristic (Ps > Pd) is due the plantation alignments which produce line gaps, and the high values of volume scattering is due to differences in branch densities, which is related to DBH density.

4. CONCLUSIONS AND RECOMMENDATIONS

The L-band backscatter attributes for three polarization modes (HH, VV and HV) from SAR R99-B/SIPAM were obtained at 13 sites of primary forest and secondary succession, in parallel with ground measurements. The relationship of SAR data and biophysical variables can be summarized as follows:

1. for similar structural conditions the primary or secondary forest cover can present different backscatter if the sampled areas are within an imaging track with variations of the incidence angle;
2. the variable tree height has a better performance to explain the backscatter, when compared to other biophysical variables, due differences in depth of vertical penetration, affecting the interaction of the microwaves with the forest because the processes of transmission, scattering and absorption that occur in different parts of the volume and/or different surfaces;
3. in a target decomposition model, the component of volumetric scattering mechanism, derived from a high branch density (a larger amount of scatterers in the resolution cell) and influenced by variations of incidence angles, has a stronger influence on the SAR response at primary and secondary forests;
4. to evaluate the best interaction between the radar signal and the biophysical parameters, the best configuration is the L and/or P band due its vertical penetration capability at low incidence angles (e.g. around 30°). On the other hand, the importance of short wavelengths is related to its ability to observe architectural properties from the forest canopy, in all possible polarizations related to all interactions (shape and orientation distribution of branches, twigs and foliages).
5. in a future investigation, analyses including a wide range of incidence angles, and analyses with Pol-InSAR data can aggregate more accurate information about biophysical parameters and its interactions.

The initial assessment, within the local level, indicate that multi-polarized airborne SAR-R99-B images, allows to understand the effects of the structural aspects at the radar response, confirming that this is a very important experiment to characterize and monitor the Amazon landscape. For studies at regional level, the Brazilian scientific community needs radar images of different polarizations and frequencies (i.e: RADARSAT-2, PALSAR/ALOS, TerraSAR, COSMO-SKYMED,

…), in order to understand the physiognomic-structural characteristics of the vegetation cover, the effects of seasonal variations which influence vegetation changes and specially the changes due to human induced processes. The above mentioned results are a basis for the analysis of a new series of polarimetric attributes from orbital SAR data, such as: the phase difference ($\Delta\varphi$), and the polarimetric coherence (γ) among polarizations; the entropy (H), the anisotropy (A) resulting from the decomposition by *eigenvalues* and *eigenvectors* of the coherence matrix [T], and the polarization response. The latter is the current route of scientific development to improve the understanding from the interaction among SAR polarimetric signals and structural parameters from the tropical forest environmental, allowing the identification of scattering mechanisms using differences in the polarization response (Figure 3) for mapping and forest inventory purposes.

Figure 3. Example of PALSAR/ALOS L-band polarimetric co-polarization response from the (a) primary forest and (b) secondary succession areas.

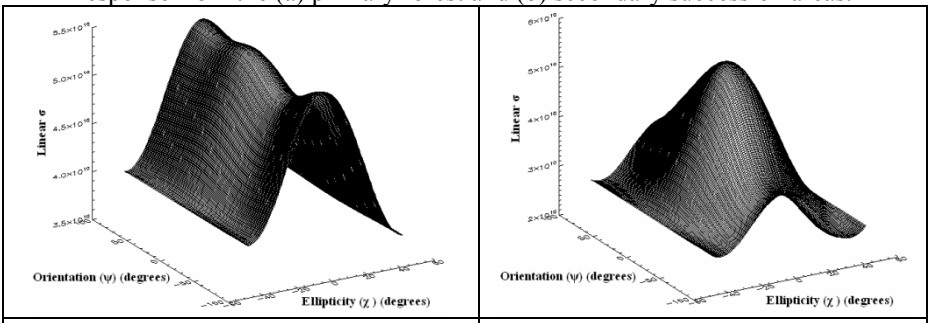

(a) (b)

Taking into account the representation in a plane ($-90º < \psi < +90º$), the highest values of intensity for an ellipticity angle at 0º and an orientation angle at 0º, the polarization is horizontally oriented (EVANS *et al.*, 1988; MC NAIRN *et al.* 2002). For the primary forest this dependence is the result of randomness of the structure with horizontal (high values around $\psi = 0°$ (horizontal polarization) and $\chi = 0°$ (linear polarization)) and vertical components ($\psi = \pm 90°$ (vertical polarization) and $\chi = 0$ (linear polarization)). For the secondary succession, possibly this dependence is the result of a structure with a more homogeneous canopy and most twigs of trees that compose the upper stratum are oriented horizontally, as shown by the right values to $\chi = 0°$ and $\psi = 0°$. In a recent work by SANTOS *et al*. (2009) there is advancement on the analysis of polarimetric responses from tropical forests, with a wide range of typologies which can aggregate more knowledge about the SAR response and it interactions.

ACKNOWLEGMENTS

Thanks to CENSIPAM and LBA. The research was also funded by research grants provided by CNPq.

REFERENCES

AIBA, H.; MURATA, K; IWASHITA, H. *Experimental results of L-band microwave penetration properties of tropical and subtropical trees*. In: Proceedings of the 8th Japan Conference on Remote Sensing. p.51-54. 1988.

BALTZER, H. Forest mapping and monitoring with inteferometric synthetic aperture radar (INSAR). *Progress in Physical Geography*, v. 25, n.2, p. 159-177, 2001.

BROWN, S.; GILLESPIE, A. J. R.; LUGO, A. E. Biomass estimation methods for tropical forest with applications to forest inventory data. *Forest Science*, v. 35, p.881-902, 1989.

CHAMPION, I.; GUYON, D.; RIOM, J. Effect of forest thinning on the radar backscattering coefficient at L-band. *International Journal of Remote Sensing*, v.19, n.11, p. 2233-2238, 1998.

CLOUDE, S. R.; POTTIER, E. An entropy based classification scheme for land application of polarimetric SAR. *IEEE Transactions on Geoscience and Remote Sensing*, v.35, n.1, p. 68-78, 1997.

COOPS, N. C. Eucalyptus forest structure and synthetic aperture radar backscatter: a theoretical analysis. *Trees*, v.16, p. 28-46, 2002.

EVANS, D. L.; FARR, T. G.; VAN ZYL, J. J; ZEBKER, H. A. Radar polarimetry: analysis tools and applications. *IEEE Transactions on Geoscience and Remote Sensing*, v.26, n.6, p.774 – 789. 1988

FREEMAN, A.; DURDEN, S. L. A. Three component scattering model for polarimetric SAR data. *IEEE Transactions on Geoscience and Remote Sensing*, v.36, n.3, p. 963-973, 1998.

GRAY, A. L.; VACHON, P. W.; LIVINGSTONE, C. E.; LUKOWSKI, T. L. Synthetic Aperture Radar calibration using reference reflectors. *IEEE Transactions on Geoscience and Remote Sensing*, v.28, n. 3, p.374-383, 1990.

HAJNSEK, I.; KUGLER, F.; SEUNG-KUK LEE, S. K.; PAPATHANASSIOU, K. P. Tropical forest parameter estimation by means of Pol-InSAR: The INDREX-II campaign. *IEEE Transactions on Geoscience and Remote Sensing*, v.47, n.2, p. 481-493. 2009.

HENDERSON, F. M.; LEWIS, A. J. *Manual of remote sensing: principles and applications of imaging radars*. 3.ed. New York: John Wiley and Sons, Inc., 1998. 866 p.

HOEKMAN, D. H.; QUIÑONES, M. J. Land cover type and biomass classification using Air SAR data for evaluation of monitoring scenarios in the Colombian

Amazon. *IEEE Transactions on Geoscience and Remote Sensing*, v.38, n.2, p. 685-696, 2000.

KASISCHKE, E. S.; MELACK, J. M.; DOBSON, M. C. The use of imaging radar for ecological applications: a review. *Remote Sensing of Environment*, v.59, n.2, p.141-156. 1997.

IMHOFF, M.; STORY, M; VERMILLION, C.; KAHN, F.; POLCLYN, F. Forest canopy characterization and vegetation penetration assessment with space-borne radar. *IEEE Transactions on Geoscience and Remote Sensing*, v.GE-24, n. 4, p.535-542. 1986.

LI-WEN, Z.; XIAO-GUANG, Z.; YONG-MEI, J.; GANG-YAO, K. *Iterative classification of polarimteric SAR image based on the Freeman decomposition and scattering entropy. Synthetic Aperture Radar, 2007 - APSAR 2007*. 1st Asian and Pacific Conference. Huangshan, China, 5-9 Nov., 2007. p.473-476. 2007.

MC NAIRN, H.; DUGUAY, C.; BRISCO, B.; PULTZ, T. Z. The effect of soil and crop residue characteristics on polarimetric radar response. *Remote Sensing of Environment*, v.80, n.2, p.308-320. 2002.

MOUGIN, E.; PROISY, C.; MARTY, G.; FROMARD, F.; PUIG, H.; BETOULLE, J. L.; RUDANT, J. P. Multifrequency and multipolarization radar backscattering from mangrove forests". *IEEE Transactions on Geoscience and Remote Sensing*, v. 37, n.1, p. 94-102, 1999.

NEEFF, T.; DUTRA, L. V.; SANTOS, J. R. FREITAS, C. C.; ARAÚJO, L. S. Power spectrum analysis of SAR data for spatial forest characterization in Amazônia. *International Journal of Remote Sensing*, v. 26, n.13, p. 2851-2865, 2005.

SAATCHI, S. S.; SOARES, J. V.; ALVES, D. S. Mapping deforestation and land use in Amazon rainforest by using SIR-C imagery. *Remote Sensing of Environment*, v.59, p. 191-202. 1997.

SANTOS, J. R.; NARVAES, I. S.; GRAÇA, P. M. L. A.; GONÇALVES, F. G. Polarimetric responses and scattering mechanisms of tropical forest in the Brazilian Amazon. In: *Advances in Geoscience and Remote Sensing*, Ed. Gary Jedlovec. InTech, Vulkovar, Croatia. Cap.8, 2009. p. 183-206.

SANTOS, J. R.; PARDI LACRUZ, M. S.; ARAUJO, L. S.; KEIL, M. Savanna and tropical rainforest biomass estimation and spatialization using JERS-1 data. *International Journal of Remote Sensing*, v.23, n.7, p. 1217-1229, 2002.

TREUHAFT, R. N.; CHAPMAN, B.; DUTRA, L.V.; GONÇALVES, F. G.; SANTOS, J. R.; MURA, J. C.; GRAÇA, P. M. L. A.; DRAKE, J. Estimating 3-dimensional structure of tropical forest from radar interferometry. *Ambiência*, v. 2, n.1, p.111-119, 2006.

Uhl, C.; BUSCHBACHER, R.; SERRÃO, E. A. S. Abandonned pastures in eastern Amazonia. I: patterns of plant sucession. *Journal of Ecology*, v.76, p. 663-681, 1998.

VAN DER SANDEN, J. J. *Radar remote sensing to support tropical forest management*. Wageningen, The Netherlands (Wageningen Agricultural University), Tropenbos-Guyana Series 5, doctoral thesis, 330 p. 1997.

VAN ZYL, J. J. Unsupervised classification of scattering behavior using radar polarimetry data", *IEEE Transactions on Geoscience and Remote Sensing*, v. 27, p. 36-45, 1989.

VAN ZYL, J. J., ZEBKER H. A., ELACHI, C. Imaging radar polarimetric signatures: theory and observation. *Radio Science*, v. 22, n.4, p. 529-543, 1987.

WATANABE, M.; SHIMADA, M.; ROSENQVIST, A.; TADONO, T.; MATSUOKA, M.; ROMSHOO, A. A.; OHTA, K.; FURUTA, R.; NAKAMURA, K.; MORIYAMA, T. Forest structure dependency of the relation between L-Band σ0 and biophysical parameters. *IEEE Transactions on Geoscience and Remote Sensing*, v. 44, n.11, p. 3154-3165, 2006.

ZHANG, L.; ZHANG, J.; ZOU, B.; ZHANG, Y. *Comparison of methods for target detection and applications using polarimetric SAR image*. PIERS Online, v. 4, n.1, 2008. p. 140-145.

(Recebido em dezembro de 2009. Aceito em maio de 2010).